



Search for $H \rightarrow \gamma\gamma$ produced in association with top quarks and constraints on the Yukawa coupling between the top quark and the Higgs boson using data taken at 7 TeV and 8 TeV with the ATLAS detector



ATLAS Collaboration ^{*}

ARTICLE INFO

Article history:

Received 10 September 2014
 Received in revised form 21 November 2014
 Accepted 25 November 2014
 Available online 2 December 2014
 Editor: W.-D. Schlatter

Keywords:

Higgs boson
 Diphoton decay
 $t\bar{t}H$
 Top quark
 Yukawa coupling
 tH

ABSTRACT

A search is performed for Higgs bosons produced in association with top quarks using the diphoton decay mode of the Higgs boson. Selection requirements are optimized separately for leptonic and fully hadronic final states from the top quark decays. The dataset used corresponds to an integrated luminosity of 4.5 fb^{-1} of proton–proton collisions at a center-of-mass energy of 7 TeV and 20.3 fb^{-1} at 8 TeV recorded by the ATLAS detector at the CERN Large Hadron Collider. No significant excess over the background prediction is observed and upper limits are set on the $t\bar{t}H$ production cross section. The observed exclusion upper limit at 95% confidence level is 6.7 times the predicted Standard Model cross section value. In addition, limits are set on the strength of the Yukawa coupling between the top quark and the Higgs boson, taking into account the dependence of the $t\bar{t}H$ and tH cross sections as well as the $H \rightarrow \gamma\gamma$ branching fraction on the Yukawa coupling. Lower and upper limits at 95% confidence level are set at -1.3 and $+8.0$ times the Yukawa coupling strength in the Standard Model.

© 2014 The Authors. Published by Elsevier B.V. This is an open access article under the CC BY license (<http://creativecommons.org/licenses/by/3.0/>). Funded by SCOAP³.

1. Introduction

After the decades-long search for the Higgs boson [1–3], a particle consistent with the Standard Model (SM) Higgs boson has been discovered at the Large Hadron Collider (LHC) [4,5]. A notable property of the SM Higgs boson is its predicted large Yukawa coupling to top quarks, Y_t^{SM} . The measurement of Y_t is particularly important for understanding electroweak symmetry breaking and allows for testing theories beyond the SM (BSM).

The value of Y_t is indirectly tested by measurements sensitive to gluon fusion, ggF, the dominant Higgs boson production mechanism at the LHC, which receives large contributions from loop diagrams involving the top quark. In addition, Y_t is probed in the decay of the Higgs boson to two photons, $H \rightarrow \gamma\gamma$, as the decay width also involves loop diagrams with top quarks [6]. However, Y_t can be directly measured in the production of top–antitop quark pairs, $t\bar{t}$, in association with a Higgs boson [7–11], $t\bar{t}H$.

The production of the Higgs boson in association with a single top quark, tH ,¹ is also sensitive to Y_t . Three processes contribute to tH production [12–16]: t -channel ($tHqb$) production, WtH pro-

duction and s -channel tH production. The s -channel production is neglected in this Letter due to the much smaller cross section compared to $tHqb$ and WtH production. Examples of Feynman diagrams for $tHqb$ and WtH production are shown in Fig. 1.

In the SM, tH production is suppressed by the destructive interference between t -channel diagrams with Higgs bosons emitted from top quark and W boson lines, as for example shown in Fig. 1 (a) and Fig. 1 (b). In BSM theories [13–16], however, Y_t can have non-SM values, and in particular the relative sign between Y_t and g_{HWW} , which quantifies the coupling between the Higgs boson and the W boson, can be different from the SM prediction, which could lead to constructive instead of destructive interference in tH production. Hence, the tH production cross section is not only sensitive to the magnitude of Y_t but, in contrast to $t\bar{t}H$ production, it is also sensitive to the relative sign of Y_t with respect to g_{HWW} . A scale factor, κ_t , is introduced to describe the relation between Y_t and its SM value: $Y_t = \kappa_t Y_t^{\text{SM}}$. Values of $\kappa_t \neq 1$ imply modifications of the Brout–Englert–Higgs mechanism and are assumed here to leave the top quark mass and decay properties unchanged. Furthermore, only SM particles are assumed to contribute to the decay width of the Higgs boson.

This Letter reports a search for $H \rightarrow \gamma\gamma$ in association with top quarks using data recorded with the ATLAS detector [18]. Measurements in the $H \rightarrow \gamma\gamma$ decay channel are challenging due to the

^{*} E-mail address: atlas.publications@cern.ch.

¹ For simplicity, tH refers equally to $\bar{t}H$ in this Letter.

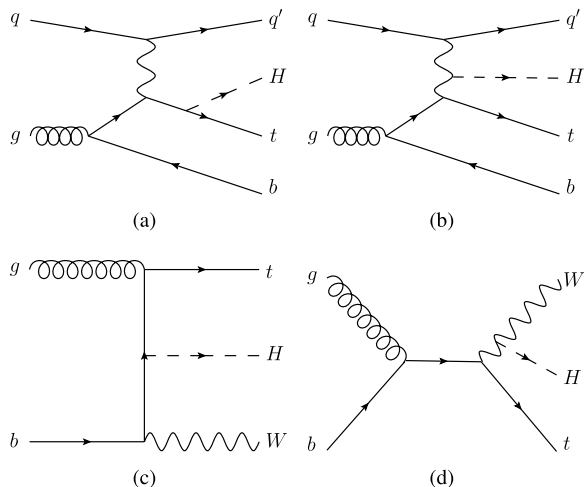


Fig. 1. Feynman diagrams showing examples for $tHqb$ (a, b) and WtH production (c, d). Higgs boson radiation off top quark and W boson lines is depicted. The $tHqb$ process is shown in the four-flavor scheme where no b -quarks are assumed to be present in the proton [17].

small branching fraction in the SM, $\text{BR}(H \rightarrow \gamma\gamma) = 2.28 \times 10^{-3}$ for Higgs boson masses, m_H , around 125 GeV. However, the diphoton final state allows the diphoton invariant mass, $m_{\gamma\gamma}$, to be reconstructed with excellent resolution, strongly reducing the contribution from the backgrounds, which have a falling $m_{\gamma\gamma}$ spectrum, referred to as continuum background in the following. The contribution from the continuum background can be derived from data sidebands, thus not relying on theory assumptions. A previous search for $t\bar{t}H$ production by the CMS Collaboration has explored hadronic, diphoton and leptonic final states of the Higgs boson [19], setting an upper limit at the 95% confidence level (CL) on the ratio of the observed $t\bar{t}H$ production cross section to the SM expectation, called the signal strength $\mu_{t\bar{t}H}$, of 4.5.

This Letter also reports lower and upper limits at 95% CL on κ_t , taking into account the changes in the $t\bar{t}H$ and tH cross sections as well as the $H \rightarrow \gamma\gamma$ branching fraction [14–16]. BSM theories with values of $Y_t \neq Y_t^{\text{SM}}$ are hence constrained.

2. The ATLAS detector

The ATLAS detector consists of an inner tracking detector system, electromagnetic and hadronic calorimeters, and an external muon spectrometer. Charged particles in the pseudorapidity² range $|\eta| < 2.5$ are reconstructed with the inner tracking detector, which is immersed in a 2 T axial field provided by a superconducting solenoid, and consists of pixel and microstrip semiconductor detectors, as well as a straw-tube transition radiation tracker. The solenoid is surrounded by sampling calorimeters, which span the pseudorapidity range up to $|\eta| = 4.9$. High-granularity liquid-argon (LAr) electromagnetic calorimeters are present up to $|\eta| = 3.2$. Hadronic calorimeters with scintillator tiles as active material cover $|\eta| < 1.74$, while LAr technology is used for hadronic calorimetry from $|\eta| = 1.5$ to $|\eta| = 4.9$. Outside the calorimeter system, air-core toroids provide a magnetic field for the muon

spectrometer. Three stations of precision drift tubes and cathode strip chambers provide a measurements of muon tracks in the region $|\eta| < 2.7$. Resistive-plate and thin-gap chambers provide muon triggering capability up to $|\eta| < 2.4$. A detailed description of the ATLAS detector can be found in Ref. [18].

3. Data and Monte Carlo samples

3.1. Data samples

Data used for this analysis were recorded in pp collisions at $\sqrt{s} = 7$ TeV and 8 TeV in 2011 and 2012, respectively. All events satisfy data quality requirements ensuring proper functioning of the detector and trigger subsystems. The resulting datasets correspond to integrated luminosities of 4.5 fb^{-1} and 20.3 fb^{-1} , respectively [20]. For the 7 TeV dataset, events were triggered with a diphoton trigger with a threshold of 20 GeV on the transverse energy of each photon candidate. For the 8 TeV dataset, these thresholds were raised to 35 GeV for the highest- E_T (leading) photon candidate and 25 GeV for the second-highest- E_T (subleading) photon candidate.

3.2. Monte Carlo samples

The contribution from the continuum background is directly estimated from data. All processes involving $H \rightarrow \gamma\gamma$ decays, however, are estimated using Monte Carlo (MC) simulation samples.

The production of $t\bar{t}H$ events is modeled using next-to-leading-order (NLO) matrix elements obtained with the HELAC-One-loop package [21], where POWHEG-BOX [22–24] is interfaced to PYTHIA 8.1 [25] for showering and hadronization. CT10 [26] parton distribution functions (PDF) and the AU2 underlying event tune [27,28] are used. Production of $tHqb$ is simulated with MADGRAPH [29] in the four-flavor scheme with the CT10 PDF set, which provides a better description of the kinematics of the spectator b -quark than the five-flavor scheme [17]. PYTHIA 8.1 is used for showering and hadronization. Production of WtH is simulated in the five-flavor scheme by MADGRAPH5_AMC@NLO [30] interfaced to Herwig++ [31] using the CT10 PDF set. All tH samples are produced for three different values of κ_t : -1 , 0 and $+1$. In the simulation of $t\bar{t}H$, $tHqb$ and WtH processes, diagrams with Higgs bosons radiated in the top quark decay are not taken into account because such contributions are negligible [32].

Higgs boson production by ggF and vector-boson fusion (VBF) is simulated with POWHEG-BOX [33,34] interfaced to PYTHIA 8.1 for showering and hadronization with CT10 PDF. Production of a Higgs boson in association with a W or Z boson (WH , ZH) is simulated with PYTHIA 8.1 using CTEQ6L1 [35] PDF.

All MC samples are generated at $m_H = 125$ GeV and are passed through a full GEANT4 [36] simulation of the ATLAS detector [37]. The simulated samples have additional pp collision events, pile-up, simulated by PYTHIA 8.1 added and weighted such that the average number of interactions per bunch-crossing is the same as in data.

The cross sections for $t\bar{t}H$ production were calculated at NLO in quantum chromodynamics (QCD) [7,9,38,39]. The cross sections for $tHqb$ production are calculated for different values of κ_t at LO using MADGRAPH with the renormalization and factorization scales set to 75 GeV, and with a minimum $p_{T,q}$ requirement of 10 GeV, consistent with the generated MC samples. LO-to-NLO K-factors are obtained by comparing the LO cross sections with the NLO cross sections calculated using MADGRAPH5_AMC@NLO. The cross sections for WtH production are calculated for different values of κ_t at NLO using MADGRAPH5_AMC@NLO with dynamic renormalization and factorization scales. Interference effects with $t\bar{t}H$ production are not considered, but are believed to be small given

² ATLAS uses a right-handed coordinate system with its origin at the nominal interaction point (IP) in the centre of the detector and the z -axis along the beam pipe. The x -axis points from the IP to the centre of the LHC ring, and the y -axis points upward. Cylindrical coordinates (r, ϕ) are used in the transverse plane, ϕ being the azimuthal angle around the beam pipe. The pseudorapidity is defined in terms of the polar angle θ as $\eta = -\ln \tan(\theta/2)$. The transverse momentum is defined as $p_T = p \sin \theta = p / \cosh \eta$, and the transverse energy E_T has an analogous definition.

Download English Version:

<https://daneshyari.com/en/article/1852810>

Download Persian Version:

<https://daneshyari.com/article/1852810>

[Daneshyari.com](https://daneshyari.com)